GeoScience Engineering

NUMERICAL SIMULATION OF ADDED MASS FORCE AND PRESSURE GRADIENT FORCE TO PREDICT THE DEPOSITION PROCESS OF PARTICLES AND THE DISTRIBUTION OF WATER VELOCITIES IN SEWERAGE PIPELINES

Farida MERROUCHI[1] *, Ali FOURAR*[2] *, Fawaz MASSOUH*[3] *, Somia LAKHDARI*[4]*, Abdelatif ZEROUAL*[1]
1 *University of Oum El Bouaghi, Faculty of Science and Applied Science, Hydraulic Department, Oum El Bouaghi, Algeria*
2 *University of Batna2, Faculty of Technology, Hydraulic Department, Batna, Algeria.*
3 National School of Arts and Crafts, Paris, France
4 Abbes Laghrour Khenchela University, Natural and life sciences, Khenchela, Algeria
E-mail: farida.merrouchi@univ-oeb.dz

ABSTRACT

The dispersion and deposition of solid particles in turbulent flows within sewer networks were numerically analyzed. Given the high density ratio between solid particles and water (greater than 0.1), observed in the semi-arid regions of Algeria, the added mass forces and pressure gradient were integrated into the particle motion equation. A coupled Euler-Lagrange approach, based on the *k-ω-SST* turbulence model and the Discrete Random Walk (DRW) model, was used to simulate fluid flow and particle transport, as well as their interaction with turbulence. The pressure gradients from the numerical simulations of turbulent flow were compared with experimental data from the Dyn-Fluid laboratory at ENSAM Paris, showing excellent agreement. The simulations revealed that pressure drop increases with particle size and higher flow velocities. They also showed that particle deposition rates correspond to known deposition zones in sewer networks, and that an increase in water velocity reduces particle deposition, in line with scientific literature.

Keywords: Euler-Lagrange modeling; Particle deposition; Pressure gradients, Sewer networks; Turbulent flow.

1 INTRODUCTION

Wastewater management is a crucial challenge in modern urban infrastructure, particularly in arid and semi-arid regions such as Algeria, where hydrological conditions are often unstable and can lead to sediment accumulation in sewer systems. In these systems, suspended solid particles are transported by turbulent flows, and their deposition can cause blockages in pipes, reducing the efficiency of drainage systems and increasing maintenance costs (Bertrand-Krajewski et al., 2000). Understanding the dynamics of particles in these networks is therefore essential for optimizing the management and performance of sanitation infrastructure (Dufresne et al., 2009).

Recent studies on particle dispersion in turbulent flows indicate that several factors influence deposition rates, including particle size, density, and flow velocity (Yao and Fairweather, 2012; Mu et al., 2020; Merrouchi, 2023). The density ratio between solid particles and the fluid plays a significant role in their dynamic behavior, affecting particle distribution and deposition in pipelines (Merrouchi, 2023). Moreover, recent research has demonstrated that added mass forces and pressure gradients must be integrated into simulation models to accurately represent particle behavior in complex liquid flows (Fuchs and Sutugin,1965; Maxey and Riley, 1983) For instance, Akermann et al. (2022) used the Euler-Lagrange approach to simulate particle deposition in turbulent sewer flows, showing that particle size and pressure gradients play a key role in preferential deposition zones.

In addition, Merrouchi et al. (2023) applied discrete random walk models coupled with the Euler-Lagrange approach to better understand particle behavior in turbulent flows. They demonstrated that integrating particle-turbulence

Vol. 71 (2025), No. 1
pp. 1–17, ISSN 1802-5420
DOI 10.35180/gse-2025-0115

interactions into simulations improves the accuracy of deposition predictions, especially in pipelines. Murali et al. (2019) also highlighted the importance of pipe geometry, showing that curved or constricted areas promote sediment accumulation, an essential factor to consider in modeling.

Many experimental and numerical studies have been conducted to better understand the phenomena of particle transport and deposition in turbulent flows within sewer networks. For instance, Zaza et al. (2021) employs Direct Numerical Simulations coupled with Lagrangian particle tracking to investigate the influence of the added-mass factor on the preferential concentration of particles denser than the fluid in the one-way coupling regime. It is shown how the added-mass factor affects particle distribution within the channel through the statistical correlations between particle concentration and typical descriptors of the flow topology.

Other studies, such as Akermann et al. (2023), used the Euler-Lagrange approach to simulate particle deposition in sewer pipes, demonstrating that particle size and pressure gradients play a crucial role in forming preferential deposition zones. Moreover, Merrouchi et al. (2019) showed that integrating particle-turbulence interactions through a discrete random walk model improves the accuracy of deposition predictions in complex networks.

Murali et al. (2019) analyses the magnitude of excess solids deposition due to changing wastewater composition and evaluates current approaches to modelling sewer solids. Gaps in commonly used modelling approaches for deposited bed processes, specifically in bed consolidation and bed particle cohesion processes, and gross solids transport were identified and addressed to enable better solids risk prediction and management. Finally, Monadi et al. (2023) proposed a multiphase modeling approach to predict the behavior of solid particles in complex sewer systems, validating the use of numerical simulations for sediment management in urban networks.

In this context, and due to the crucial importance of hydrodynamic conditions and particle properties, this study adopts a coupled Euler-Lagrange approach using the Discrete Particle Model (DPM). This method incorporates complex hydrodynamic forces, such as added mass forces and pressure gradients, as well as the physical characteristics of the particles, particularly their large size and high density, which significantly influence their behavior in flows. These particles, in the context of combined sewers that collect both wastewater and stormwater, present a particular challenge for modeling.

The Euler-Lagrange approach enables precise modeling of particle transport and deposition in turbulent sewer flows, accounting for their interaction with the turbulent field. To do so, we used the k-ω-SST turbulence model (Wilcox, 1988), recognized for its ability to capture the characteristics of shear flows, as well as the Discrete Random Walk (DRW) method, which provides a better understanding of particle dispersion and deposition mechanisms.

The significance of this study lies in its ability to provide a more realistic and detailed modeling of deposition processes under complex hydrodynamic conditions, such as those encountered in sewer systems in arid and semi-arid regions. The results contribute to improving sewer network management by reducing the risk of blockages caused by particle deposits while optimizing system performance under varying flow conditions and with particles of large sizes and high densities.

The average pressure gradients obtained from the numerical solution of fully developed turbulent flow, incorporating solid particles of different diameters and densities, were compared with experimental data from the Dyn-Fluid laboratory at ENSAM Paris. The simulations showed excellent agreement with the experimental results, thus validating the ability of the Euler-Lagrange model with DPM to effectively predict the trajectory and deposition of solid particles in preferential zones of sewer pipes.

2 METHODOLOGY

2.1 Governing Equations

In this work, the Euler-Lagrange approach is used for modeling particle transport. The liquid phase is simulated by solving the averaged Navier-Stokes equations, coupled with a closure model to represent dynamic Reynolds stresses.

The motion of a particle in a fluid is described from a Lagrangian perspective by solving a system of differential equations along the particle's trajectory.

Vol. 71 (2025), No. 1
pp. 1–17, ISSN 1802-5420
DOI 10.35180/gse-2025-0115

2.1.1 Continuous Phase

The Navier-Stokes equations for unsteady turbulence can be written in Cartesian coordinates

Conservation of mass equation

$$\frac{\partial \rho_f}{\partial t} + \vec{\nabla} \cdot \left(\rho_f \overrightarrow{u_f} \right) = 0 \quad (1)$$

Conservation of momentum equation

$$\frac{\partial}{\partial t}\left(\rho_f \overrightarrow{u_f} \right) + \vec{\nabla} \cdot \left(\rho_f \overrightarrow{u_f} \overrightarrow{u_f} \right) = -\nabla p + \nabla . \left(\bar{\bar{\tau}}_f^{"} + \bar{\bar{\tau}}_f^{"} \right) + \rho_f \vec{g} + \vec{s}_M \quad (2)$$

where

u_f is the velocity vector, $\bar{\bar{\tau}}_f^{"}$ is the shear stress tensor. The subscript *f* denotes the carrier fluid, ρ_f is the density of the continuous phase in kg/m^3; u_f represents the fluid velocity in m/s; p indicates the fluid pressure in Pa; $\rho_f \vec{g}$ is the gravitational body force, $\vec{s}_M$ is the added momentum due to the solid phase.

To complete the calculation, we used the low and high Reynolds number model $k-\omega$-sst, which combines the benefits of the two approaches ($k-\varepsilon$; $k-\omega$) and includes a mixing function F_1 that goes from $k-\omega$ in the near-wall zones (low Reynolds number) to $k-\varepsilon$ free flow (fully developed flow). The literature has proven that the $k-\omega$ -sst model is able to describe the boundary layer perfectly near the walls (Gilles, 2016).

The transport equations of the $k-\omega$ -sst model for unsteady, incompressible flow are formed by obtaining the corresponding turbulent kinetic energy equation k and the turbulent frequency equation ω.

$$\frac{\partial}{\partial t}(\rho k) + \frac{\partial}{\partial x_i}(\partial k u_i) = \frac{\partial}{\partial x_i}\left(\Gamma_k \frac{\partial k}{\partial x_j} \right) + \tilde{G}_k + Y_k + S_k \quad (3)$$

$$\frac{\partial}{\partial t}(\rho \omega) + \frac{\partial}{\partial x_i}(\partial \omega u_i) = \frac{\partial}{\partial x_i}\left(\Gamma_\omega \frac{\partial \omega}{\partial x_j} \right) + \tilde{G}_\omega + Y_\omega + S_\omega \quad (4)$$

In these equations, $\tilde{G}_k$ represents the production of turbulent kinetic energy due to mean velocity gradients, $\tilde{G}_\omega$ represents the generation of the dissipation frequency ω, Γ_k and Γ_ω are the effective diffusivity of k and ω, Y_k and Y_ω represent the dissipation of k and ω due to turbulence, and S_k and S_ω are source terms defined by the user.

2.1.2 Discrete Particle Motion Model

The trajectory of the particles is determined by integrating the motion equation within a Lagrangian framework. In the context of particle tracking, we make the following assumptions: (1) the injected particles are generally considered independent, and interactions between them are neglected. By also neglecting mass transfer phenomena, we introduce a large number of particulate pollutants to study the effects of particle size, density, and velocity on sedimentation. The tested particles include glass beads and alumina beads. The governing equation of particle motion is formulated according to Newton's second law

$$\frac{d\vec{x}_p}{dt} = \vec{u}_p \quad (5)$$

where $\vec{x}_p$ and $\vec{u}_p$ present respectively the position vector and the velocity vector of the particle,

The particle velocity u_p can be calculated by solving the force balance on the particle, which is expressed as:

$$\frac{d\vec{u}_p}{dt} = f_{Dp}\left(\vec{u}_f - \vec{u}_p\right) + \vec{g}\left(\frac{\rho_p - \rho_f}{\rho_i}\right) + \vec{f}_p + \vec{f}_{vm} + \vec{f}_{interaction,p} \quad (6)$$

The first term on the right-hand side represents the drag force acting on an individual particle, where u_f is the velocity of the fluid phase and u_p is the velocity of the particle. f_{Dp} is defined in the relationship below.

Vol. 71 (2025), No. 1
pp. 1–17, ISSN 1802-5420
DOI 10.35180/gse-2025-0115

$$f_{Dp} = \frac{\mu_f}{\rho_p dp_i^2} \frac{18 C_{Dp} Re_{pi}}{24} \quad (7)$$

where the drag coefficient C_D is calculated by the correlations of Morsi and Alexander (1972)

$$C_D = \frac{k_1}{Re_p} + \frac{k_2}{Re_p^2} + k_3 \quad (8)$$

The particle Reynolds number presented in relation (8) is calculated by the formula below.

$$Rep_i = \frac{d_{pi} \rho_f \alpha_f |\vec{u}_f - \vec{u}_p|}{\mu_f} \quad (9)$$

$\vec{f}_p$, $\vec{f}_{vm}$ represent the pressure gradient force and added mass force the expressions of which are given as:

$\vec{f}_p$ is the force due to pressure gradient: $F_p = \left(\frac{\rho_f}{\rho_p}\right)\left(\vec{u}_f \nabla \vec{u}_f\right)$ (10)

$\overrightarrow{f_{vm}}$ is the virtual mass force: $\vec{f}_{vm} = C_{vm} \frac{\rho_f}{\rho_p}\left(\frac{d\vec{u}_f}{dt} - \frac{d\vec{u}_p}{dt}\right)$ (11)

where C_{vm} is the virtual mass factor with a default value of 0.5, since varying its value has no influence on the calculation results. The last term $\vec{f}_{interaction,i}$ represents the additional acceleration acting on a single particle from the interaction between the particles, which is calculated from the stress tensor of KTGF (the kinetic theory of granular flow).

$$\vec{f}_{interaction,p} = -\frac{1}{\rho_p} \cdot \nabla . \overline{\overline{\tau}}_i \quad (12)$$

2.1.3 Two-Way Coupling of Fluid and Dispersed Phases in Particle-Laden Flows

The coupling between the two phases, the carrier fluid and the dispersed phase, is crucial for understanding their dynamic interaction. The carrier fluid acts on the dispersed phase by exerting drag forces and generating turbulence, while the particles in the dispersed phase influence the fluid by reducing its mean momentum and turbulence. To model this interaction, a two-way coupling is employed, where particle source terms are integrated into the Navier-Stokes equations to account for these mutual effects.

2.1.4 Modeling Particle Dispersion in Turbulent Flows: The DRW Approach

In our study, we simulated the dispersion of particles in a turbulent flow using the stochastic method called the DRW (Discrete Random Walk) random walking models. The lifespan and size of the vortices are calculated by informing the Lagrangian time constant, C_L. This is the only parameter of the model. In the case of K -ω-SST, the Lagrangian time value, T_L is calculated by:

$$T_L = C_L \frac{K}{0.09 K \omega} \quad (13)$$

where K is the turbulent kinetic energy and ω is the specific dissipation rate of the turbulent kinetic energy.

3 NATURE AND POSITION OF THE PROBLEM

3.1 Flow Configuration and Simulation Set-up

Figure 1 illustrates the geometry of the computational domain, representing a test pipe similar to the unit-type main pipe supplying the Ain-Beida wastewater treatment plant, located in the wilaya of Oum El Bouaghi, Algeria. This horizontal pipe has an internal diameter of D = 100 mm and a length of 10 m. (Additional information about the test

Vol. 71 (2025), No. 1
pp. 1–17, ISSN 1802-5420
DOI 10.35180/gse-2025-0115

setup can be found in the study by F. Ravelet, et al. (2013). The model is designed to simulate the flow of a carrier fluid containing solid particles.

The simulations involve solid particles, specifically glass and alumina beads, with sizes ranging from 5 mm and 6 mm and densities between 2 500 kg/m³ and 3 650 kg/m³. The fluid, flowing through the pipe at average speeds of 1, 2, 3, 4 m/s, replicates the real flow conditions observed in the wastewater systems of the region

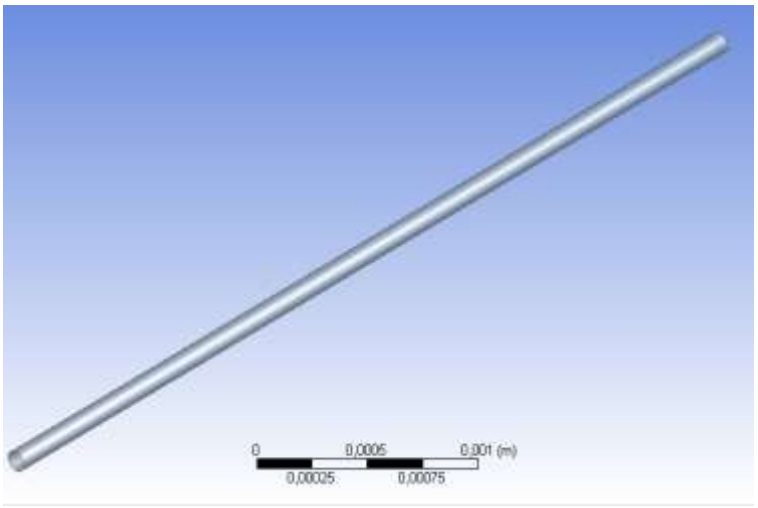

Figure 1. *Geometry of the pipe.*

3.2 Characteristics of solids Particles in Turbulent Flow

In order to analyze the impact of the sizes and densities of solid particles on the hydrodynamic behavior of turbulent flows in sewer systems, while incorporating hydrodynamic forces such as pressure gradient force and added mass force, simulations were carried out.

These simulations consider a mixture of solid particles of varying sizes and densities (as shown in Table 1) as the particulate phase, with water as the continuous phase. The inlet velocities of the mixture, calculated based on the volumetric flow passing through the pipe section, were defined for different scenarios to better understand the interactions between the particles and the fluid.

Table 1*. Physical characteristics of solid particles and different mixtures*

Types	Glass Beads	Alumina Beads	Mixture 1 (Alumina)	Mixture 3 (Alumina / Glass)	Water
Diameter (mm)	5	6	50% 5 mm glass beads with 50% 6 mm alumina	50% 5 mm glass beads with 50% 6 mm alumina	
Density (kg/m^3)	2 500	3 650	3 075	2 500 and 3 650	998.2
Viscosity ($Ns/m^{2)}$	0.001003	0.001003	0.001003	0.001003	0.001003

4 CFD MODELING

4.1 Mesh Configuration in 3-D Computational Domain

The 3D computational domain used in this study is generated through a detailed meshing process, including surface meshing and volume meshing (see Figure 2). Special attention is given to surface grids due to their significant impact on the overall quality of the volume grids. To ensure accuracy in the flow field, particularly near the pipe walls, a finer grid resolution is applied in the boundary layer. The mesh configuration includes approximately 910,000 cells in total.

Vol. 71 (2025), No. 1
pp. 1–17, ISSN 1802-5420
DOI 10.35180/gse-2025-0115

The mesh generated for this study consists of a structured grid applied to the cross-sectional surfaces and a non-structured hexagonal mesh for the entire volume. A mesh sensitivity analysis was performed to ensure that beyond a certain number of cells, increasing mesh density does not significantly influence accuracy. In this case, a mesh size of around 910,000 cells was found to be optimal, balancing computational cost with simulation precision.

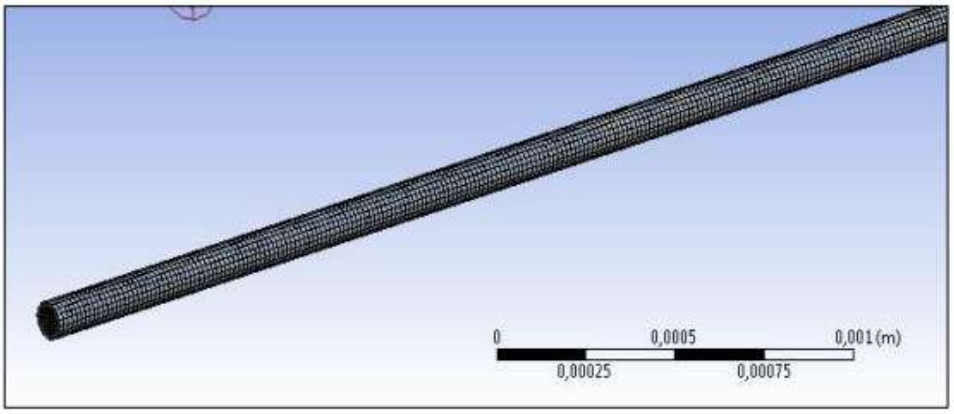

Figure 2. *3D mesh of the mipe*

4.2 Simulation Parameters and Methodology

For this study, the numerical simulations were conducted using ANSYS Fluent software to solve the set of equations through the finite volume method, employing a second-order implicit scheme in both time and space. ANSYS Fluent offers great flexibility in choosing discretization schemes for each governing equation. A double-precision solver for pressure and velocity was used by applying the pseudo-transient method along with the coupled algorithm. The PRESTO! pressure solver method was selected to enhance convergence while maintaining high accuracy.

For the pressure terms, standard discretization schemes were applied, while second-order discretization schemes were adopted for the convection terms to ensure greater accuracy in the results. The convergence criteria for all unsteady simulations were set such that the residual in each control volume is smaller than 10^{-6} or the number of iterations reaches 1000.

Regarding the discrete phase model (DPM), the number of continuous phase iterations per DPM iteration is set at 10. The boundary conditions for the model are outlined in Table 2.

Table 2*. Boundary conditions for water and particulate phase*

Water	Inlet water (velocity inlet) Outlet water (pressure outlet) Wall of the conduit (wall)
Particulate pollutants	«Escape »: The particles exited the computation domain $\frac{\partial \bar{u}}{\partial x} = \frac{\partial \bar{v}}{\partial x} = \frac{\partial \bar{w}}{\partial x} = 0,$ Lateral wall of the pipe: « Reflect »: The particles bounce off the borders with a change of direction following the coefficient of restitution Bottom wall of the pipe« Trap »: The trajectory calculations are terminated and there is no changing in the sediment surface

5 CFD SIMULATION RESULTS

In this section, we present the results of 3D numerical simulations aimed at analyzing the dispersion and deposition of solid particles in turbulent flows within sewer pipelines. The main objective of this study is to assess the influence of added mass forces, pressure gradients, and the physical properties of particles on particulate transport in pipelines, particularly in semi-arid regions where the density ratio between solid particles and water exceeds 0.1. Additionally, this study examines the hydrodynamic behavior of water within these pipelines.

Vol. 71 (2025), No. 1
pp. 1–17, ISSN 1802-5420
DOI 10.35180/gse-2025-0115

Simulations were conducted to test the sensitivity of the results to particle characteristics, such as diameter and density. For all simulations, the Eulerian-Lagrangian approach (DPM) was adopted to model particle transport, using the $K-\omega-SST$ turbulence model for the fluid phase dynamics. The dispersion model employed a stochastic Discrete Random Walk (DRW) method to capture particle trajectories in turbulent flow. The total number of particles simulated was set at 455,272, with a division of 0.006, ensuring the accuracy and representativeness of the results.

5.1 Numerical Validation of the DPM Model for Particle Transport in Sewer Pipelines

In this section, the validity of the results obtained with the DPM model is verified by comparing the calculated hydraulic gradients with experimental data from Zouaoui et al. (2016) and Ravelet et al. (2013). The numerical simulations aim to analyze the behavior of particles in sewer pipelines, taking into account the influence of hydrodynamic forces.

The DPM model is based on a Eulerian-Lagrangian approach to model the transport of solid particles, integrating the effects of added mass forces, pressure gradients, and the physical properties of the particles. The results demonstrate a good agreement between the simulated values of the hydraulic gradient and the experimental data, proving the effectiveness of the models used to predict particle transport in pipelines, particularly in semi-arid environments. The numerical validation thus confirms the reliability of the simulations, ensuring an accurate representation of the hydrodynamic behavior of water and solid particles (See Figures 3, 4, 5, 6 and 7).

5.1.1 Analysis of the Effects of Mixing Velocity and Particle Properties on the Hydraulic Gradient Considering Added Mass and Pressure Forces

The study of the effects of mixing velocity and particle properties on the hydraulic gradient, conducted through numerical simulations at the Dyn-Fluid laboratory of ENSAM Paris, reveals complex and interconnected dynamics that influence the behavior of loaded fluids. The results demonstrate that the introduction of solid particles, such as alumina with a diameter of 6 mm or glass with a diameter of 5 mm, or a mixture of both (alumina and glass), systematically increases the hydraulic gradient compared to that of pure water (Figure 8). This phenomenon is primarily attributed to the increase in the effective viscosity of the fluid when solid particles are present.

The analysis of Figures (3, 7) shows that the hydraulic gradient is sensitive to the mixing velocity. At velocities below 2 m/s, the effect on the hydraulic gradient for the 6 mm particle is marginal, indicating a certain inertia of the system in response to low mixing velocities. In contrast, once the threshold of 2 m/s is exceeded, the impact on the hydraulic gradient becomes significant, illustrating a more dynamic response of the flow to variations in mixing velocity. This suggests that interactions between solid particles and the fluid are intensified at higher velocities, modifying turbulence and thereby increasing the pressure drop in the conduits.

This study highlights the importance of added mass forces and pressure gradients in the behavior of loaded fluids. The interaction between solid particles and the liquid leads to accumulated turbulence, which in turn affects the pressure drop within the system. The results of the simulations are consistent with the experimental data from Ravelet et al. (2013) and Zouaoui et al. (2016), confirming the validity of the DPM model in predicting particle transport. However, a minor divergence is observed compared to models that do not account for added mass forces and pressure gradient forces, emphasizing the importance of these factors in understanding the behavior of loaded fluids in conduits.

In conclusion, this analysis demonstrates that mixing velocity and particle characteristics have significant effects on the hydraulic gradient, and that models incorporating hydrodynamic forces provide a better representation of the phenomenon, enabling more effective management of sanitation systems and conduits in various environments.

5.1.2 Integrated Impact of Forces and Particle Diameters on Hydraulic Gradient in Complex Flows

In Figure 3, where only the added mass force is considered, it is observed that the hydraulic gradient reaches a maximum value at a mixing velocity of 1 m/s, before decreasing to 0.12 at a velocity of 2 m/s. Beyond this velocity,

Vol. 71 (2025), No. 1
pp. 1–17, ISSN 1802-5420
DOI 10.35180/gse-2025-0115

the hydraulic gradient increases again, reaching a value of 0.18 at a mixing velocity of 4 m/s. This variation suggests a direct impact of the particles on the effective fluid density and flow resistance.

In comparison, Figure 4, which illustrates the effect of the pressure gradient with 6 mm particles, also shows a notable rise in the hydraulic gradient. This indicates that the increase in pressure within the system enhances particle transport, thereby strengthening hydraulic resistance in the conduits. These results highlight the importance of considering these forces for an accurate modeling of particle behavior in turbulent flows.

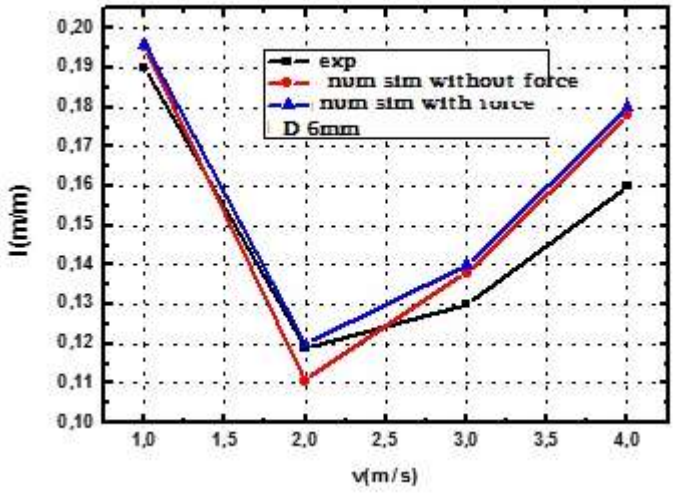

Figure 3. *Comparison profile of the hydraulic gradient simulated by the DPM model and experimental results (Ravelet et al.,2013; Zouaoui et al.,2016) as a function of mixing velocity (effect of added mass force)*

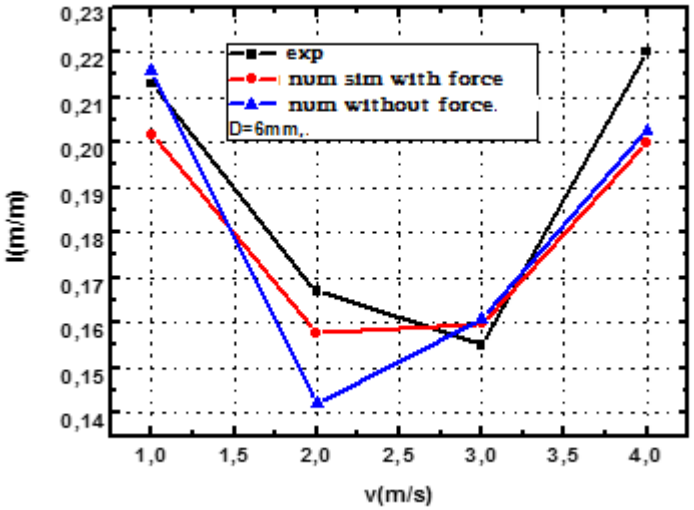

Figure 4. *Comparison profile of the hydraulic gradient simulated by the DPM model and experimental results (Ravelet et al.,2013; Zouaoui et al.,2016) as a function of mixing velocity (ffect of pressure gradient)*

In Figure 5, which integrates both the added mass force and the pressure gradient force, a clear synergy emerges between these two factors, resulting in a significantly elevated hydraulic gradient. This indicates that the combined effect of the added mass and pressure gradient forces enhances resistance to flow, highlighting the complex interactions that occur when both forces are at play. This interaction amplifies turbulence and modifies the effective viscosity of the fluid, leading to a more pronounced impact on flow behavior compared to considering each force individually.

Vol. 71 (2025), No. 1
pp. 1–17, ISSN 1802-5420
DOI 10.35180/gse-2025-0115

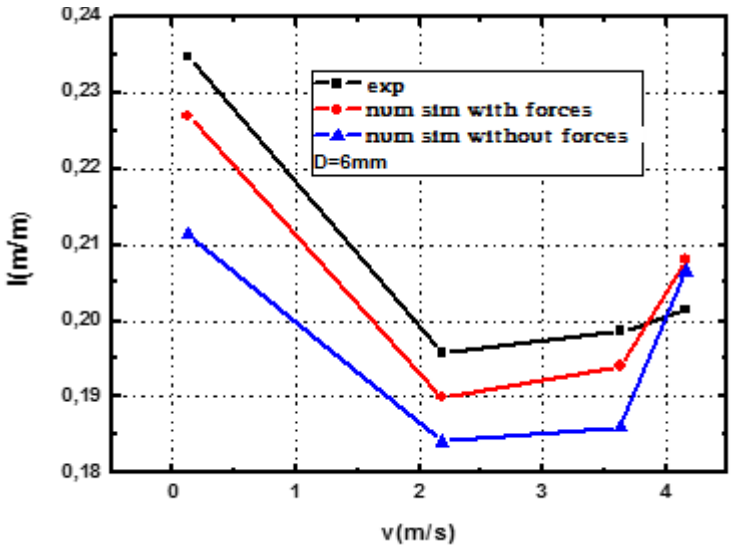

Figure 5. *Comparison profile of the hydraulic gradient simulated by the DPM model and experimental results (Ravelet et al.,2013; Zouaoui et al.,2016) as a function of mixing velocity (effect of added mass force and pressure gradient)*

Moving on to Figure 6, which analyzes 5 mm diameter particles while accounting for both forces, it is observed that the hydraulic gradient is influenced by the complex interactions between particle size and the acting forces. Additionally, the increase in hydraulic gradient with velocity suggests a dynamic response of the system as both the particle size and forces contribute to resistance within the flow.

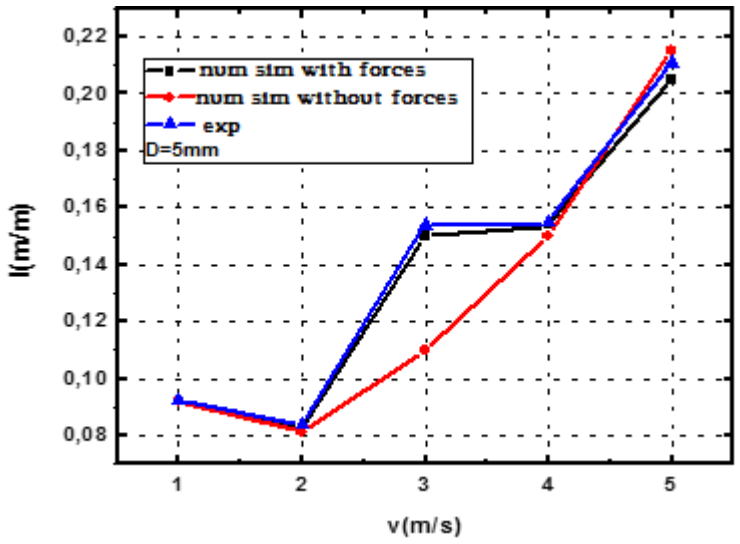

Figure 6. *Comparison profile of the hydraulic gradient simulated by the DPM model and experimental results (Ravelet et al.,2013; Zouaoui et al.,2016) as a function of mixing velocity (effect of added mass force and pressure gradient)*

In Figure 7, which combines both forces and both particle diameters, it is demonstrated that the variation in particle diameter, in conjunction with the forces, further amplifies the hydraulic gradient. This highlights the need for an integrated approach to understanding the behavior of particle-laden flows. These results illustrate that both the added mass force and the pressure gradient are critical for accurately modeling and predicting hydraulic behavior in pipelines, especially under complex flow conditions.

Vol. 71 (2025), No. 1
pp. 1–17, ISSN 1802-5420
DOI 10.35180/gse-2025-0115

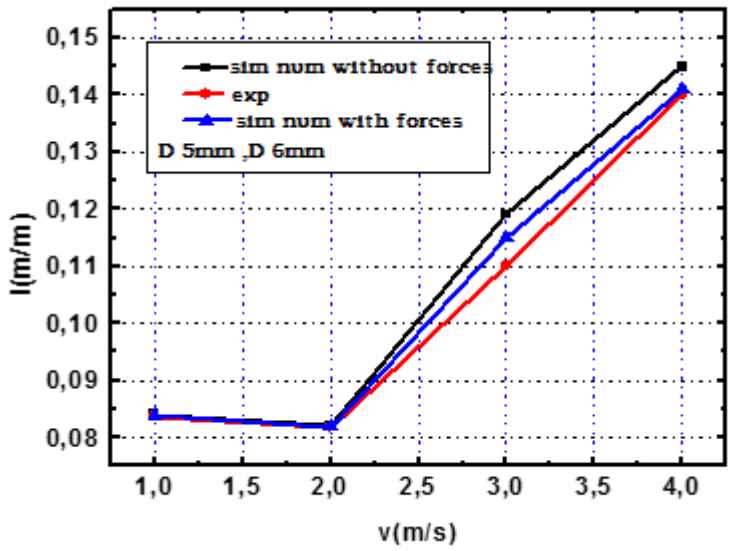

Figure 7. *Comparison profile of the hydraulic gradient simulated by the DPM model and experimental results (Ravelet et al.,2013; Zouaoui et al.,2016) as a function of mixing velocity (effect of added mass force and pressure gradient)*

5.1.3 Influence of Particle Properties

In this section, we will examine the influence of particle properties, such as density and size, on the hydraulic gradient. The numerical results for pressure drop for two types of solids (alumina and glass), with diameters of 5 and 6 mm and respective densities of 2500 kg/m³ and 3650 kg/m³, are presented in Figure 8. We observe that the increase in density leads to a significant rise in pressure losses. The numerical results closely align with those of Ravlet et al. (2013) and Zouaoui et al. (2016.

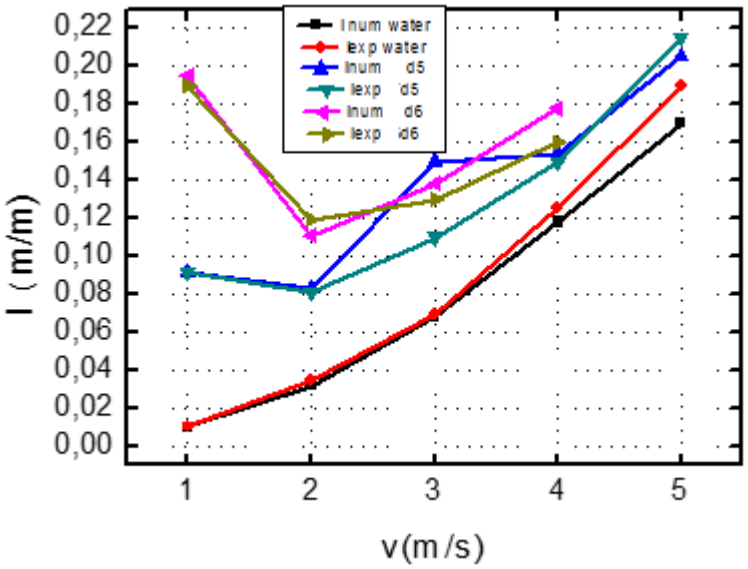

Figure 8. *Hydraulic gradient as a function of mixing velocity considering density effects and particle diameters of glass and alumina with the inclusion of forces*

Vol. 71 (2025), No. 1
pp. 1–17, ISSN 1802-5420
DOI 10.35180/gse-2025-0115

5.2 Impact of Particle Properties on Flow Dynamics in Sewer Networks

To precisely illustrate the influence of solid particle properties on the velocity field of liquid flow in a combined sewer pipeline, test series were selected to represent two distinct weather conditions: dry weather and rainy weather. Numerical simulations were conducted with different velocities imposed at the inlet of the pipeline: one corresponding to a low flow rate, representing wastewater-only flow (Figure 5), and higher velocities simulating heavy rain conditions (wastewater combined with rainwater, Figure 6), with respective values ranging from 1 m/s to 5 m/s.

5.2.1 Analysis of Euler-Lagrange Models for Solid Particles under Rainy Conditions (D = 5 mm)

The results obtained using the Euler-Lagrange models (DPM) for 5 mm solid particles under rainy conditions reveal a significant trend: as we move radially towards the center of the pipe, an increase in axial velocity is observed, especially at higher velocities (see Figure 9). This behavior has been corroborated by previous studies such as those by Wang et al. (2014), who also identified a similar dynamic in turbulent flows carrying solid particles.

Regarding the impact of 5 mm glass particles, it was noted that their presence slightly alters the flow, as illustrated by Figures 9,10, and 11. Although subtle, this alteration aligns with the findings of Zouaoui et al. (2016, who highlighted a similar influence of solid particles on flow profiles. Furthermore, the increase in flow velocity leads to a greater suspension of glass beads. These results highlight the importance of particle-fluid interactions, which influence not only the velocity distribution but also the suspension mechanisms within the pipes.

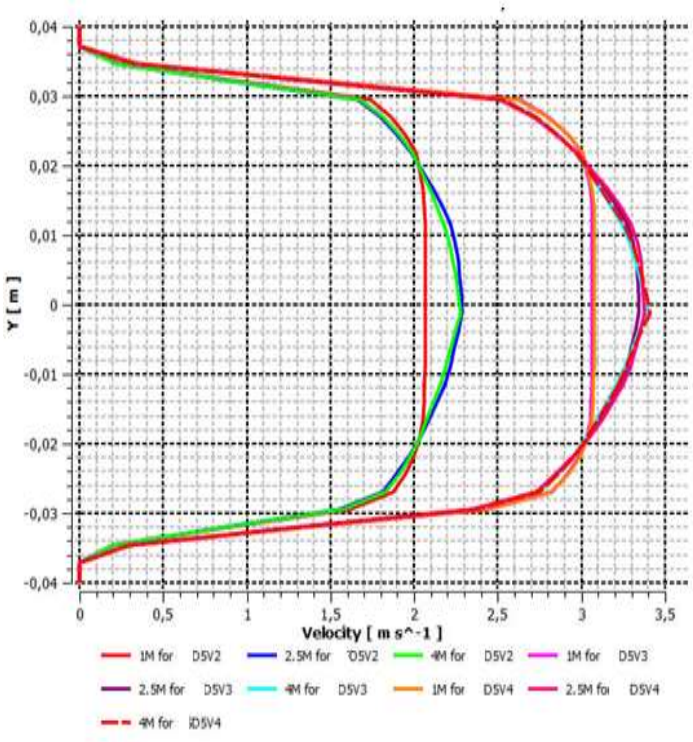

Figure 9. *Representation of velocity profiles at different axial distances (Z = 1, 2.5, and 4 m) for different mixing velocities (2, 3, and 4 m/s) under rainy conditions over 30 s*

Vol. 71 (2025), No. 1
pp. 1–17, ISSN 1802-5420
DOI 10.35180/gse-2025-0115

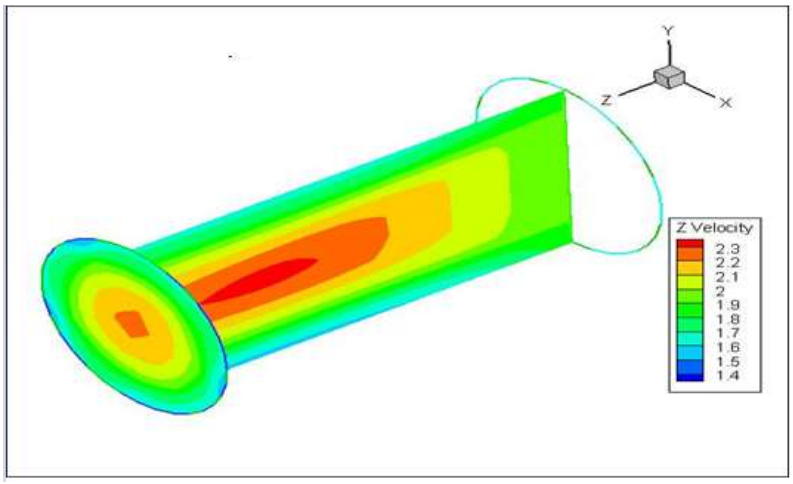

Figure 10. *Distribution of liquid phase velocity in m/s at different planes (outlet, median perpendicular) for vm = 2 m/s*

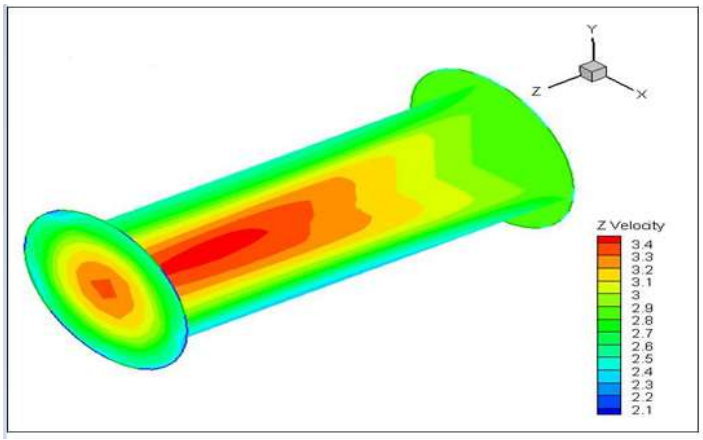

Figure 11. *Distribution of liquid phase velocity in m/s at different planes (inlet, outlet, median, parallel, and perpendicular) for vm = 4 m/s*

Regarding the particulate phase, Figure 12 illustrates the influence of particles on the average flow of this phase within the pipe. The results show that the injection of solid particles at a concentration corresponding to rainy conditions and a mixing velocity of 4 m/s induces an increase in turbulence. This turbulence promotes better mixing of fluid and solid particles, as demonstrated in Figure 12. This observation aligns with what is typically seen in the real pipeline (Figure 12) and is also consistent with previous findings published by Zheng et al. (2020).

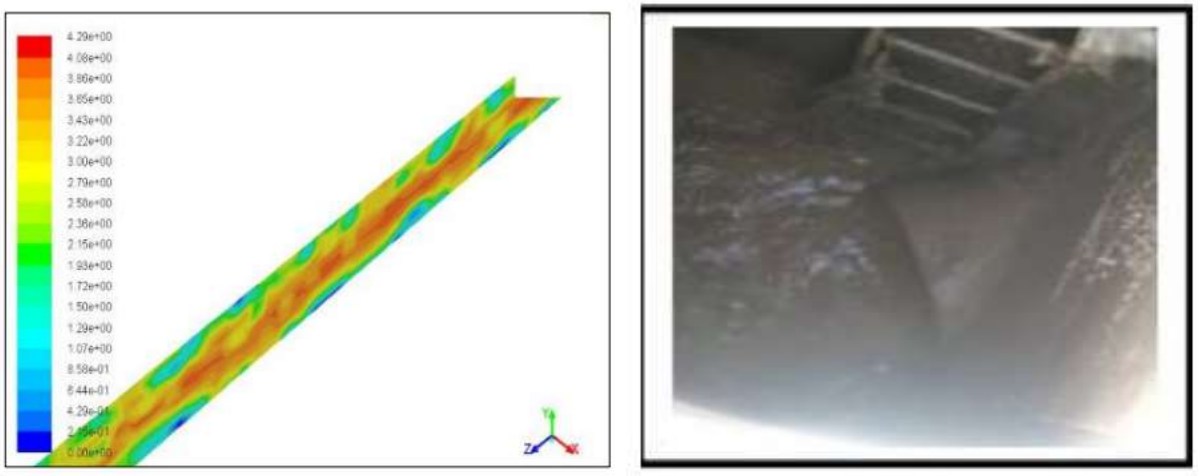

Figure 12. *Qualitative observation of the liquid-solid flow in the pipe (reality and simulation for rainy weather.*

Vol. 71 (2025), No. 1
pp. 1–17, ISSN 1802-5420
DOI 10.35180/gse-2025-0115

5.2.2 Analysis of Euler-Lagrange Models for Solid Particles under Dry Conditions (D = 5 mm)

We can observe that for low velocities on the order of 1 m/s (Figures 13, 14), the level of turbulence is not sufficiently high, causing the particles to tend to accumulate at the bottom of the pipe. The numerical simulations qualitatively reproduce the asymmetrical nature of the average velocities of the particulate phase in the pipe, as they show particle deposition in the lower part of the pipe (Figures 13,14).

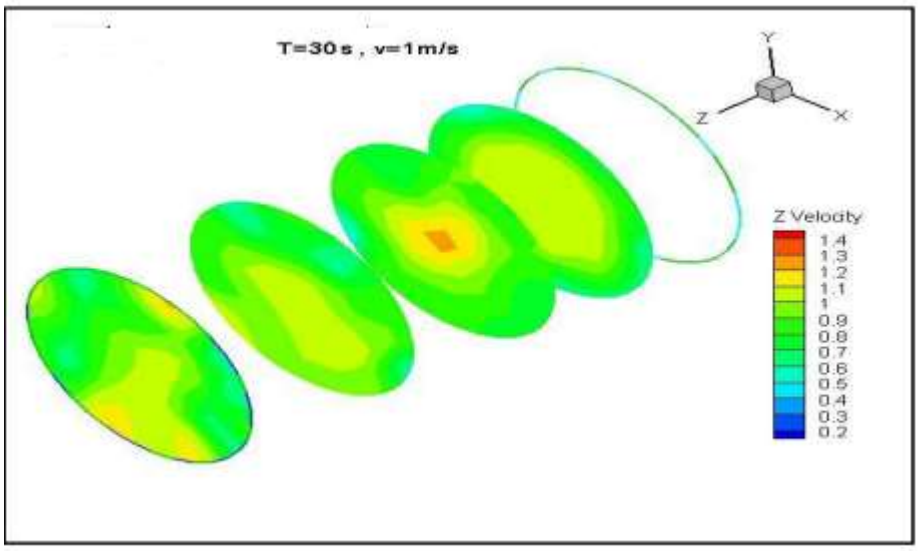

Figure 13. *Distribution of axial velocity in m/s of the liquid phase at different axial distances in the pipe for mixing velocities of 1 m/s (dry conditions)*

For flows in sewer pipes at low mixing velocities, superimposed flow regimes are observed, with an underlying regime loaded with compact particles forming a deposition zone where velocities are negligible. As the mixing velocity decreases, solids tend to deposit, as seen in dry conditions (Figure 14). In different sections of the horizontal pipe, various flow regimes are observed, including one with a stationary layer of solids resting at the bottom of the pipe. The numerical simulations were in agreement with the actual observations (Figure 14) and consistent with the specialized literature, including the works of Zheng et al. (2020), Wang et al. (2020), and Li et al. (2019).

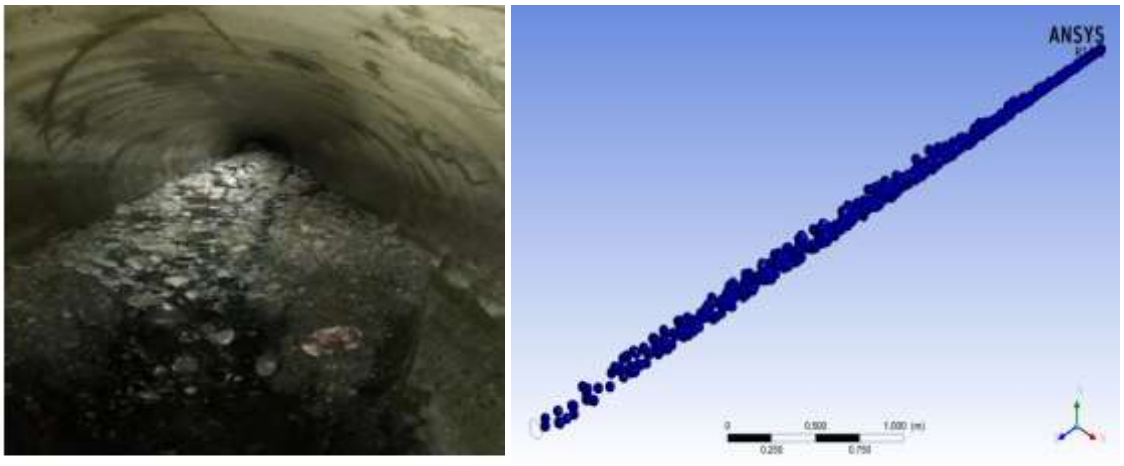

Figure 14. *Qualitative observation of the liquid-solid flow in the pipe (reality and simulation for dry weather)*

5.2.3 Analysis of Euler-Lagrange Models for Solid Particles under Rainy and Dry Conditions (D = 6 mm)

Vol. 71 (2025), No. 1
pp. 1–17, ISSN 1802-5420
DOI 10.35180/gse-2025-0115

Figure 15 shows that under rainy conditions, the presence of particles in the fluid leads to a significant increase in axial velocity. This velocity reaches a maximum value at the center of the pipe, while a slowdown is observed in the lower part, due to the accumulation and deposition of particles in this area.

However, as the mixing speed increases, a symmetry of velocities is noted. This change is attributed to the increase in turbulence, which promotes a more complete mixing of solid and fluid particles. It can be emphasized that under conditions of higher concentration and speed, turbulence plays a crucial role in the redistribution of velocities within the fluid. This suggests that controlling the mixing speed could be essential for optimizing particle transport in wastewater systems.

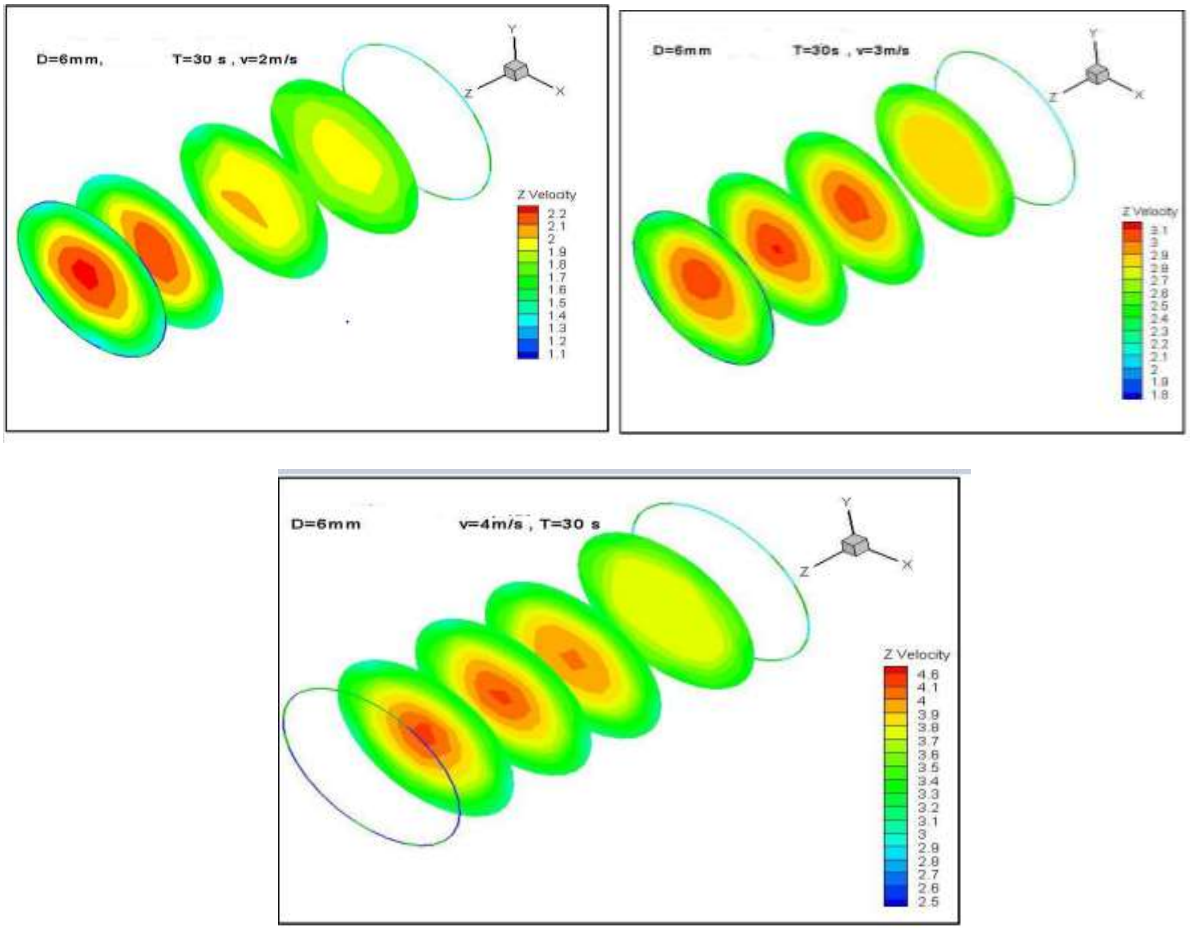

Figure 15. *Distribution of axial velocity in m/s of the liquid phase at different axial distances from the pipe for different mixing velocity (d=6 mm, rainy conditions)*

During dry periods, the flow in these pipes exhibits low mixing velocities, characteristic of superimposed flow regimes. In this context, a sub-regime is loaded with compact beads, forming a deposition zone where velocities are reduced (see Figure 16). The lower the mixing velocity, the more the solids tend to settle. Different flow regimes are observed in various sections of the pipe, including one with a stationary layer of solids resting at the bottom. These results are consistent with those experimentally obtained by Ravelet et al. (2013), Zouaoui et al. (2016) and Yamaguchi et al. (2011). These flow regimes are also marked by a significant pressure drop, resulting from a reduction in the cross-sectional area, which leads to an increase in the velocity of the liquid phase near the upper wall (see Figure 16).

Vol. 71 (2025), No. 1
pp. 1–17, ISSN 1802-5420
DOI 10.35180/gse-2025-0115

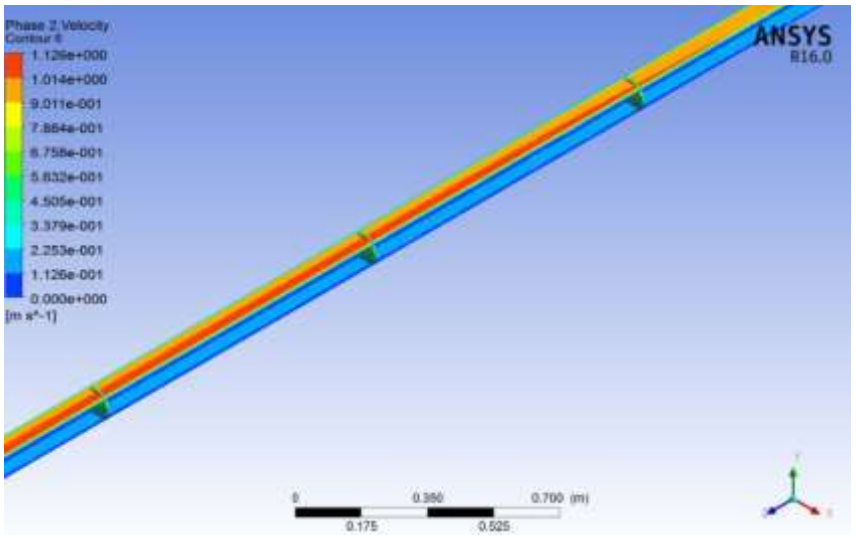

Figure 16. *Velocity distribution in m/s near the wall lane for a mixing elocity of 1 m/s for 6 mm particles*

Figure 17 shows that the Euler-Lagrange DPM model, by introducing the forces of added mass and the pressure gradient force, effectively identifies the deposition zones at the bottom of the pipe. At low velocities, the mass forces dominate, leading to the accumulation of particles at the bottom. However, while the model provides a good representation, it tends to overestimate these particle-laden zones. This can be attributed to an underestimation of the effect of particle dispersion, which could keep them suspended more than anticipated.

The accumulation of solid particles at the bottom of the pipe has significant implications for the dynamics of the flow. It can lead to changes in wall roughness and affect the velocity profile of the fluid. The accumulation may also cause variations in pressure, thereby influencing the pressure gradient throughout the flow. Consequently, the particle-laden zones can create obstructions that alter the overall flow rate and velocity distribution.

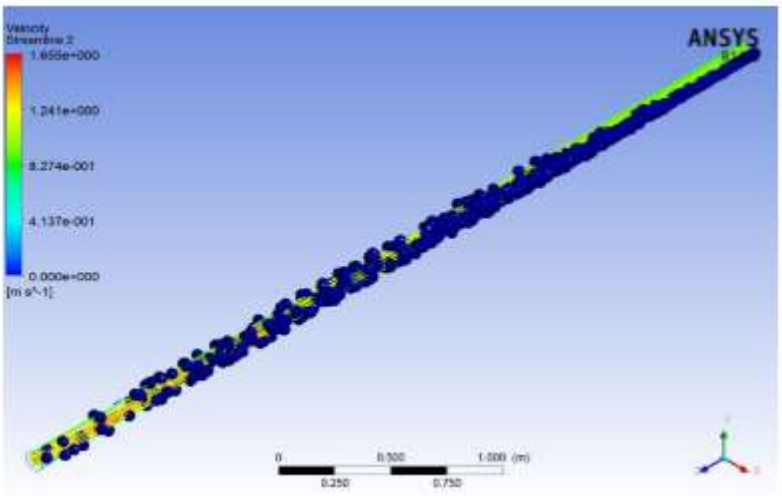

Figure 17. *Representation of the trajectory of solid particles after a duration of 30 s for vm = 1 m/s*

6 CONCLUSION

This study successfully simulated the transport and deposition of solid particles in turbulent flows within sewer networks. Using a coupled Euler-Lagrange approach with the Discrete Particle Model (DPM), we accounted for complex hydrodynamic forces such as added mass force and pressure gradient to predict particle behavior and analyze particle-turbulence interactions. The results showed a strong correlation between numerical predictions and experimental data, validating our modeling approach.

Vol. 71 (2025), No. 1
pp. 1–17, ISSN 1802-5420
DOI 10.35180/gse-2025-0115

The simulations revealed the significant impact of particle size and density on the hydraulic gradient, confirming that large and dense particles increase pressure loss and promote preferential deposition zones within the pipes. Furthermore, it was demonstrated that increasing flow velocity reduces particle deposition, which could contribute to improving sewer network management.

In conclusion, this work provides key insights into the dynamics of solid particles in turbulent flows. The results of this research offer valuable perspectives for optimizing sewer networks, particularly in semi-arid regions where hydrological conditions favor sediment accumulation. The models developed and validated in this study could be used to design more effective and sustainable solutions to prevent blockages and minimize maintenance costs in sewer systems.

REFERENCES

AKERMANN, K. and RENZE, P., 2022. Simulation of turbulent particle deposition in rough pipes using an Euler-Lagrange approach. In: *Proceedings of the 7th bwHPC Symposium*. Ulm: Universität Ulm, pp. 7–10. Available from: http://dx.doi.org/10.18725/OPARU-46057.

BERTRAND-KRAJEWSKI, J. L.; BARRAUD, S. and CHOCAT, B., 2000. Need for improved methodologies and measurements for sustainable management of urban water systems. *Environmental Impact Assessment Review*. Vol. 20, no. 3, pp. 323–331. Available from: https://doi.org/10.1016/S0195-9255(00)00044-5.

DUFRESNE, M.; VAZQUEZ, J.; TERFOUS, A.; GHENAIM, A. and POULET, J., 2009. Experimental investigation and CFD modelling of flow, sedimentation, and solids separation in a combined sewer detention tank. *Computer & Fluids*. Vol. 38, no. 5, pp. 1042–1049. Available from: https://doi.org/10.1016/j.compfluid.2008.01.011.

FUCHS, N.A. and SUTUGIN, A.G.,1965. Coagulation rate of highly dispersed aerosols. *Journal of Colloid Science*. Vol. 20, no. 6, pp. 492–500. Available from: https://doi.org/10.1016/0095-8522(65)90031-0.

GILLES, I., 2016. *Approche Euler-Lagrange pour la modélisation du transport solide dans les ouvrages de décantation.* Thèse de doctorat. INSA de Strasbourg, France.

LI, M.Z.; HE, Y.P., LIU, Y.D. and HUANG, C., 2019. Analysis of transport properties with varying parameters of slurry in horizontal pipeline using ANSYS fluent. *Particulate Science and Technology*. Vol. 38, no. 6, pp. 26–739. Available from: https://doi.org/10.1080/02726351.2019.1621412.

MAGNAUDET, J., 1997. The forces acting on bubbles and rigid particles. In: *ASME Fluids Engineering Division Summer Meeting FEDSM'97.* Vancouver, Canada. Vol. 3522, pp. 22–26

MAXEY, M.R. and RILEY, J.J., 1983. Equation of motion for a small rigid sphere in a non uniform flow. *Physics of Fluids*. 1983, vol. 26(4), pp. 883-889. Available from: https://doi.org/10.1063/1.864230

MERROUCHI, F., 2019. *Numerical modeling of the variation in velocities of unsteady turbulent flows in free surface channels*. Doctoral thesis. Batna: University of Batna 2, Algeria.

MERROUCHI, F.; FOURAR, A.; ZEROUAL, A.; MAKHLOUFI, H. and BOUZEGHAYA, A., 2023. Numerical simulation of turbulent water-solid-particle flows to predict the solid deposition process and the velocity distribution of water in sewage pipes. *Advances in Environmental Technology*. Vol. 9, no. 4, pp. 294–309. Available from: https://doi.org/10.22104/aet.2023.1331.

MONADI, M. and MOHAMMADI, M., 2023. Sedimentation in heavy laden urban combined sewer conduits using a multi-phase Eulerian-Eulerian model. *Urban Water Journal*. Vol. 20, no. 8, pp. 979–994. Available from: https://doi.org/10.1080/1573062X.2023.2229289

MORSI, S.A. and ALEXANDER, A.J., 1972. An investigation of particle trajectories in two-phase flow systems. *Journal of Fluid Mechanics*. Vol. 55, no. 2, pp. 193–208.

MU, L.; WANG, S.; ZHAI, Z.; SHANG, Y.; ZHAO, C. et al., 2020. Unsteady CFD simulation on ash particle deposition and removal characteristics in tube banks: Focusing on particle diameter, flow velocity, and temperature. *Journal of the Energy Institute*. Vol. 93, no. 4, pp. 1481–1494. Available from: https://doi.org/10.1016/j.joei.2020.01.010.

MURALI, M.K.; HIPSEY, M.R.; GHADOUANI, A. and YUAN, Z., 2019. The development and application of improved solids modelling to enable resilient urban sewer networks. *Journal of Environmental Management*. Vol. 240, pp. 219–230. Available from: https://doi.org/10.1016/j.jenvman.2019.03.120.

RAVELET, F.; BAKIR, F.; and KHELLADI, S. and REY, R., 2013. Experimental study of hydraulic transport of large particles in horizontal pipes. *Experimental Thermal and Fluid Science*. Vol. 45, pp. 187–197. Available from: https://doi.org/10.1016/j.expthermflusci.2012.11.003.

WANG, L.; GUO, J.C. and MI, Z., 2014. Drafting, kissing and tumbling process of two particles with different sizes. *Computers and Fluids*. Vol. 96, pp. 20–34. Available from: https://doi.org/10.1016/j.compfluid.2014.03.005.

WANG, S.; DING, X. and WANG, J., 2020. Numerical simulation of coarse particle pipeline transportation based on Eulerian Lagrangian model. *Journal of Physics: Conference Series*. Vol. 1600, no.1, article 012005. Available from: https://doi.org/10.1088/1742-6596/1600/1/012005.

WILCOX, D.C., 1988. Reassessment of the Scale-determining Equation for Advanced Turbulence Models. *AIAA Journal*. Vol. 26, no. 11, pp. 1299–1310.

YAMAGUCHI, H.; NIU, X.D.; NAGAOKA, S. and DE VUYST, F., 2011. Solid-Liquid Two-Phase Flow Measurement Using an Electromagnetically Induced Signal Measurement Method. *Journal of Fluids Engineering*. Vol. 133, no. 4, article 041302. Available from: https://doi.org/10.1115/1.4003856.

YAO, J. and FAIRWEATHER, M, 2012. Particle deposition in turbulent duct flows. *Chemical Engineering Science*. Vol. 84, pp. 781–800. Available from: https://doi.org/10.1016/j.ces.2012.09.020.

ZAZA, D. and IOVIENO, M., 2024. On the Preferential Concentration of Particles in Turbulent Channel Flow: The Effect of the Added-Mass Factor. *Energies*. Vol. 17, no. 4, article 783. Available from: https://doi.org/10.3390/en17040783.

ZHENG, E.; RUDMAN, M.; KUANG, S. and CHRYSS, A., 2020. Turbulent coarse-particle suspension flow: Measurement and modeling. *Powder Technology*. Vol. 373, pp. 647–659. Available from: https://doi.org/10.1016/j.powtec.2020.06.080

ZOUAOUI, S.; DJEBOURI, H.; MOHAMMEDI, K., KHELLADI, S. and AIDER, A.A., 2016. Experimental study on the effects of big particles physical characteristics on the hydraulic transport inside a horizontal pipe. *Chinese Journal of Chemical Engineering*. Vol. 24, no. 2, pp.317–322. Available from: https://doi.org/10.1016/j.cjche.2015.12.007.